ELSEVIER

Biochimica et Biophysica Acta 1509 (2000) 1–6

BIOCHIMICA ET BIOPHYSICA ACTA
BBA

www.elsevier.com/locate/bba

Rapid report

# A model of calcium channels

Ben Corry [a,b], Toby W. Allen [a], Serdar Kuyucak [b], Shin-Ho Chung [a,*]

[a] *Protein Dynamics Unit, Department of Chemistry, Research School of Physical Sciences, Australian National University, Canberra, A.C.T. 0200, Australia*

[b] *Department of Theoretical Physics, Research School of Physical Sciences, Australian National University, Canberra, A.C.T. 0200, Australia*

Received 10 July 2000; accepted 8 September 2000

**Abstract**

We propose a model of calcium channels that can explain most of their observed properties, including the anomalous mole fraction effect and mutation of the glutamate residues. The structure grossly resembles that of the KcsA potassium channel except for the presence of an extracellular vestibule and a shorter selectivity filter containing four glutamate residues. Using this model in electrostatic calculations and Brownian dynamics simulations, we study mechanisms of ion permeation and selectivity in the channel. Potential energy profiles calculated for multiple ions in the channel provide explanations of ion permeation, the block of $Na^+$ currents by $Ca^{2+}$ ions, and many other observed properties. Brownian dynamics simulations provide quantitative predictions for the channel currents which reproduce available experimental data. 

*Keywords:* Calcium channel; Modelling; Permeation; Selectivity; Brownian dynamics; Electrostatics

Calcium channels provide a communication mechanism between cells that is necessary for neurotransmission, muscle contraction and neurochemical modulation. To perform this role they must exhibit remarkable selectivity while conducting millions of ions into the cell each second [1], two properties that are difficult to reconcile. Whereas the recent determination of the structures of the KcsA potassium [2] and the MscL mechanosensitive [3] channels has led to some understanding of the structure–function relationship [4–6], a protein structure for calcium channels is yet to be produced. The challenge is, therefore, to use the available data from patch clamp and mutagenesis experiments, to propose a structure that can reproduce the extraordinary properties of this important ion channel. Here we put forward such a model, and use electrostatic calculations and Brownian dynamics (BD) simulations to examine it. We reproduce many experimental results, and provide simple explanations for these in terms of electrostatic ion–ion and ion–channel interactions.

On the basis of known experimental properties of calcium channels [7–11], primary structure [12], molecular models [13,14] and insights gathered from the structure of the potassium channel, we have constructed a three-dimensional calcium channel model, shown in the inset of Fig. 1. The important features are a wide extracellular mouth, a narrow selectivity filter ($r = 2.8$ Å) with four strongly charged glutamate

* Corresponding author. Fax: +61-2-6247-2792;
E-mail: shin-ho.chung@anu.edu.au

0005-2736/00/$ – see front matter 
PII: S0005-2736(00)00330-8

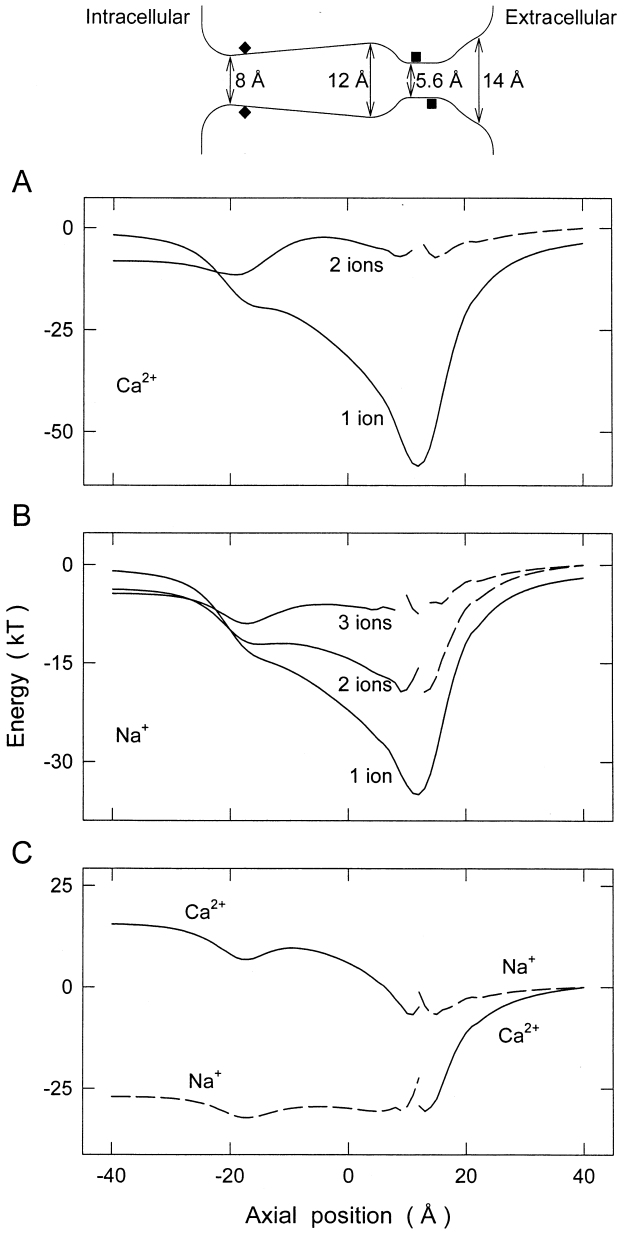


Fig. 1. Electrostatic energy profiles. The calcium channel model is generated by rotating the curves shown in the inset (top) by 180°. The positions of two of the four glutamate groups are shown by the black squares and the mouth dipoles by the diamonds. Potential energy profiles are shown for one and two $Ca^{2+}$ ions (A); one, two and three $Na^{+}$ ions (B); and the mixed case of one $Ca^{2+}$ (solid line) and one $Na^{+}$ (dashed line) ion. In all profiles the test ion is moved in 1 Å steps in the $z$ direction, and at each position allowed to move to its minimum energy position in the $x$–$y$ plane. In multi-ion profiles, the extra ions in the channel are allowed to move to their minimum energy positions at each position of the test ion. The left and right sides of the curves correspond to the test ion entering from the left or the right.

residues placed in a helical pattern, and a long chamber region that tapers toward the intracellular side. Four mouth dipoles are placed at the intracellular entrance to overcome the large image forces. The charges on the glutamates and mouth dipoles are optimized to maximize ionic currents as discussed later. The dielectric constant of the channel protein is taken as $\varepsilon_p = 2$ and water as $\varepsilon_w = 60$ [15]. While a lower value of $\varepsilon_w$ in the selectivity filter may be more appropriate, a fast solution of Poisson's equation (necessary for BD simulations) is only possible with a uniform $\varepsilon_w$ in the channel. Even with a lower value of $\varepsilon_w$, we expect to obtain similar potential energy profiles because the increased effectiveness of glutamates will be largely cancelled by their higher protonation.

In Fig. 1, we present the electrostatic potential energy profiles for various ion configurations in the channel obtained from numerical solutions of Poisson's equation using the boundary charge method [16]. A $Ca^{2+}$ ion entering an empty channel falls into a very deep potential well of 58 kT created by the glutamate charges (lower solid line in A). A second $Ca^{2+}$ ion entering from the right (corresponding to physiologically favored inward current) meets a much smaller well (7 kT, dashed line in A) and it can coexist with the first ion in a stable equilibrium. More importantly, the first $Ca^{2+}$ ion now faces a relatively small barrier on the left (5 kT, upper solid line in A), which it can surmount through random motions and cross the channel. These profiles suggest that two $Ca^{2+}$ ions are involved in the permeation process. A similar picture emerges for $Na^{+}$ ions as shown in (B) except that the channel can now hold up to three ions in a stable equilibrium. As there is a large potential well with only one or two ions in the channel we expect all three ions will be required for permeation. Also, as the barrier seen by the left-most ion in this case is only 1 kT, $Na^{+}$ should cross the channel more readily than $Ca^{2+}$. In (C) we show the profiles for the mixed case of one $Ca^{2+}$ (solid line) and one $Na^{+}$ (dashed line) ion entering the channel whilst the other inhabits the potential well. Clearly, when there is a $Na^{+}$ ion in the channel, a $Ca^{2+}$ ion can easily enter from the right and push the $Na^{+}$ out (lower curves). However, a $Na^{+}$ ion entering the channel will not be able dislodge the $Ca^{2+}$ ion because it faces an insurmountable barrier of 16 kT

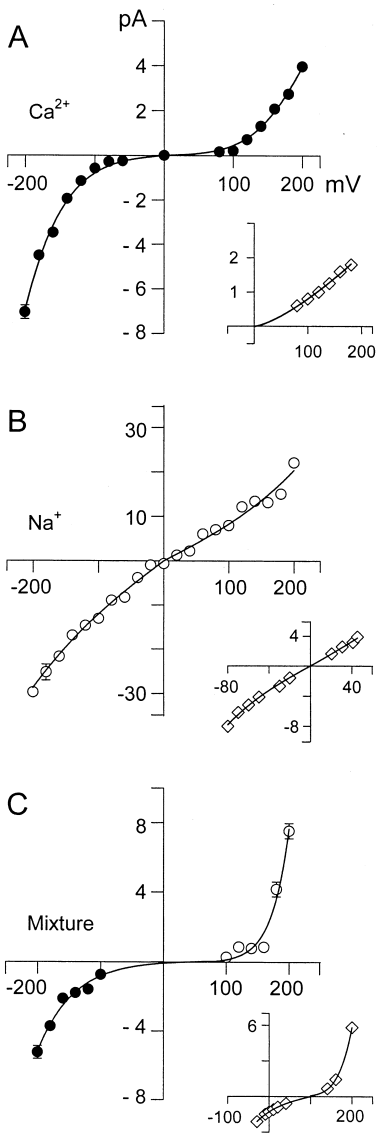


Fig. 2. Current–voltage relationships. The magnitude of the $Ca^{2+}$ (filled circles) and $Na^{+}$ (open circles) current passing through the channel from BD simulations with a symmetric solution of (A) 150 mM $CaCl_2$ and (B) 150 mM NaCl in both reservoirs, and (C) an asymmetrical mixture of 100 mM $CaCl_2$ and 50 mM NaCl on the extracellular side of the channel and 50 mM NaCl only on the intracellular side, is plotted against the strength of the driving potential. The insets show experimental data in similar conditions [19,20]. In this and following figures, error bars have a length of one standard error of the mean and are not shown when smaller than the data points.

(upper curves). A second $Na^{+}$ ion cannot enter the channel and help expel the $Ca^{2+}$ ion as it faces a steeply rising Coulomb barrier (not shown). Thus while a $Ca^{2+}$ ion can easily dislodge one or more $Na^{+}$ ions, the existence of a $Ca^{2+}$ ion in the channel blocks the permeation of $Na^{+}$ ions.

We next perform BD simulations that turn the insights derived from the electrostatic energy profiles above into quantitative predictions on various properties of the calcium channel. In these simulations we randomly place a number of ions at the desired concentration in reservoirs attached to each end of the channel and trace the motion of these ions under the influence of electric forces using the Langevin equation [15]. The channel only conducts for a narrow range of charges, and we adopt the values that maximize this current. For both the $Ca^{2+}$ and $Na^{+}$ this occurs with charges of $1.3\times10^{-19}$ C on the glutamate residues and $0.6\times10^{-19}$ C on the mouth dipoles. That we use a value slightly lower than $e$ for the glutamates is reasonable given the likelihood of protonation [17]. The diffusion coefficients of $Ca^{2+}$ and $Na^{+}$ are estimated from the molecular dynamics simulations of Allen et al. [18]. We adopt 0.5 times the bulk diffusion coefficient for $Ca^{2+}$ ions in the channel chamber ($-25 < z < 7.5$ Å) and 0.1 times the bulk value in the selectivity filter ($7.5 < z < 20$ Å). Corresponding values of 0.5 and 0.4 times the bulk value are used for $Na^{+}$. The cur-

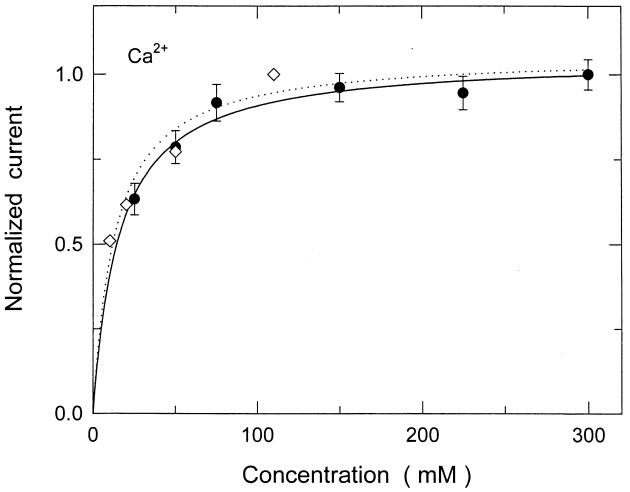


Fig. 3. Current–concentration relationships. The current obtained with symmetrical solutions of varying concentrations of $CaCl_2$ in the reservoirs is shown normalized by its value at 300 mM (normalized values are used to account for the larger driving potential required in BD simulations for reliable statistics). An applied voltage of −200 mV is used and the data points are fitted by the solid line using the Michaelis–Menten equation. Experimental data of Hess et al. [21] are shown by the open diamonds and dotted line.

rent–voltage relationships shown in Fig. 2 are obtained from BD simulations using symmetrical solutions of 150 mM $CaCl_2$ (A); 150 mM NaCl (B); and an asymmetrical mixture of 100 mM $CaCl_2$ and 50 mM NaCl on the extracellular side of the channel and 50 mM NaCl only on the intracellular side (C). Experimental results [19,20] are shown in the insets for comparison. The conductance values of $Ca^{2+}$ and $Na^{+}$ calculated at an applied potential of −120 mV in the symmetric cases are 9.7 and 122 pS, close to the experimentally determined values of 8–9 pS for $Ca^{2+}$ with 100 mM solutions and 90 pS for $Na^{+}$ in 150 mM solutions [20,21]. In all relationships, there is a small asymmetry between the inward and outward currents and a pronounced deviation from the linear Ohm's law when the applied potential is greater than ∼100 mV. This nonlinearity can also be seen in the experimental data, albeit to a slightly lesser extent. In the mixed case it can be seen that the presence of $Ca^{2+}$ blocks $Na^{+}$ current as the inward current is comprised of $Ca^{2+}$ only.

The current–concentration relationship for $Ca^{2+}$ found from BD simulations is shown in Fig. 3. These results follow closely the well known Michaelis–Menten form. The experimental results of Hess et al. [21] describing saturation of the $Ca^{2+}$ current are well reproduced by the BD simulations.

Experimental studies of mixtures of $Ca^{2+}$ and $Na^{+}$ ions in calcium channels have shown a remarkable behavior. As the relative concentration of $Ca^{2+}$ to $Na^{+}$ is decreased, the conductance of the channel first decreases to a minimum and then increases again to a maximum when there is no $Ca^{2+}$ present [22]. This so-called 'anomalous mol fraction effect'

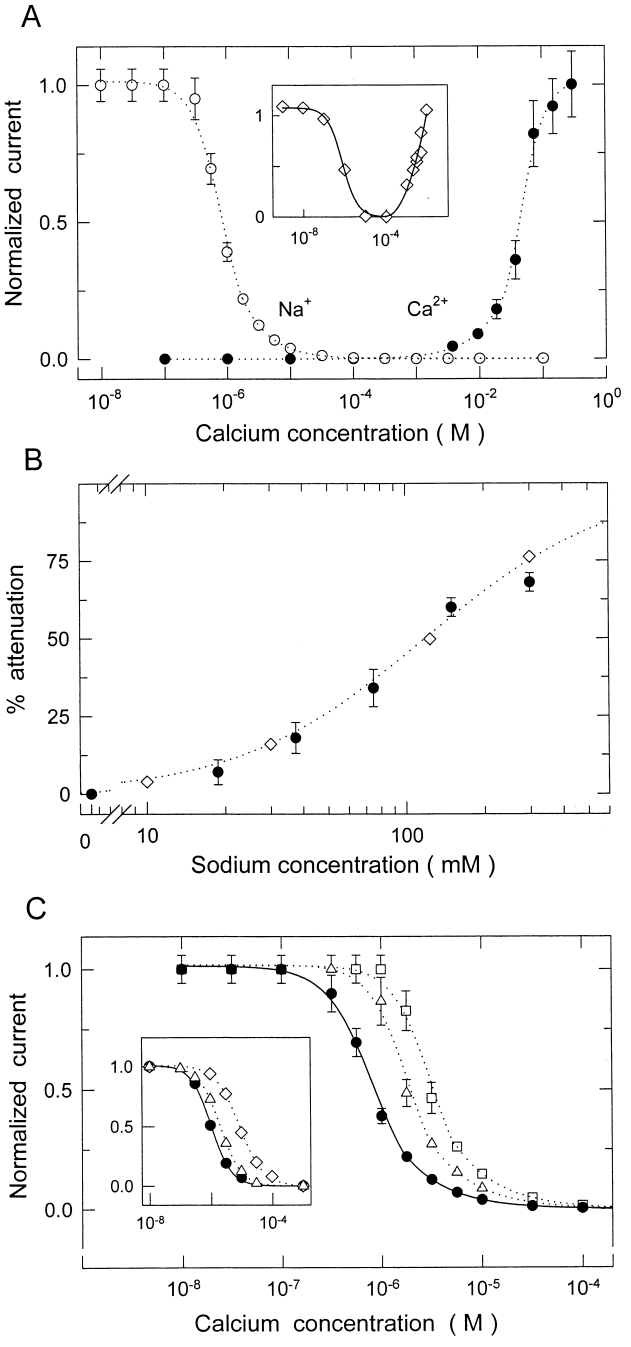


Fig. 4. Calcium channel properties with ionic mixtures under a driving potential of −200 mV. (A) Mol fraction effect. The $Ca^{2+}$ (filled circles) and $Na^{+}$ (open circles) current passing through the channel normalized by the maximum value of each is shown with different symmetrical $Ca^{2+}$ concentrations in the reservoirs. The $Na^{+}$ concentration is fixed at 150 mM in both reservoirs in all cases. Experimental results [22] are shown in the inset. (B) Attenuation of $Ca^{2+}$ current by $Na^{+}$ ions. The percentage attenuation of channel current is determined from BD simulations at different $Na^{+}$ concentrations by comparing to the value in the absence of $Na^{+}$. The $Ca^{2+}$ concentration is held at 150 mM in both reservoirs (filled circles). The open diamonds and dotted line show experimental data [25]. (C) The effect of removing glutamate charges on channel selectivity. The $Na^{+}$ current passing through the channel at different $Ca^{2+}$ concentrations with all four glutamate charges in place (filled circles), the outermost glutamate removed (triangles) and the innermost glutamate removed (squares), otherwise all conditions are as in (A). Experimental data for wild type (filled circles) and for single glutamate to glutamine mutations of two different residues (triangles and diamonds) [10] are shown in the inset.

has been a major subject of attention in calcium channel literature [1,23]. We have investigated this behavior in BD simulations by fixing the $Na^+$ concentration at 150 mM and measuring the channel current at different $Ca^{2+}$ concentrations. We extrapolate to concentrations lower than 10 mM (where we cannot complete BD simulations) using the values at higher concentrations. As seen in Fig. 4A, when the $Ca^{2+}$ concentration decreases the $Ca^{2+}$ current also decreases, as was the case in the concentration conductance curve, since it takes longer for two $Ca^{2+}$ ions to enter the channel as required for conduction. Sodium only conducts before the channel becomes blocked by a $Ca^{2+}$ ion. At lower $Ca^{2+}$ concentrations, this takes longer to occur and the $Na^+$ current increases. Experimental results [22] are shown in the inset for comparison.

A number of experimental results suggest that the presence of monovalent ions can slow the permeation of $Ca^{2+}$ ions [24,25]. We examined the effect of external $Na^+$ ions on $Ca^{2+}$ conductance by holding the $Ca^{2+}$ concentration fixed at 150 mM and varying the $Na^+$ concentration from 0 to 300 mM. The BD simulation results in Fig. 4B show that, as the $Na^+$ concentration is increased, the attenuation of $Ca^{2+}$ current also increases. The BD data points very closely reproduce the experimental results [25]. We find that this attenuation is caused by $Na^+$ ions occasionally entering and occupying the outer vestibule. Although they cannot displace a resident $Ca^{2+}$ ion from the channel, their presence does slow the entry of a second $Ca^{2+}$ ion required for conduction.

Mutations of one or more of the glutamate residues have provided many useful insights into binding and selectivity in the calcium channel. The replacement of a glutamate residue with a neutral one severely lowers the conductance of the channel for divalent ions, and to a lesser extent for monovalent ions [11]. Also, the block of monovalent currents by divalent ions is severely hampered, only arising at much higher divalent concentrations [10]. In BD simulations, we mimic the experimental site-directed mutagenesis by removing one of the charges representing the glutamate residues. In this case we find that the current is maximized when the charge on each remaining amino acid is a full $1.6\times10^{-19}$ C. That protonation should occur to a lesser degree in the mutated channel is plausible because there is less charge in the channel to attract and bind protons. In Fig. 4C we show how the selectivity of the channel for $Ca^{2+}$ over $Na^+$, and the effectiveness of $Ca^{2+}$ block, diminish when the innermost or outermost glutamate group is removed, compared to when all are present. We find that the removal of one of the glutamate groups results in $Ca^{2+}$ ions taking longer on average to enter and block the channel, meaning that $Na^+$ ions have more time to permeate and the channel becomes less selective. The experimental data [10] shown in the inset exhibit a similar shift in selectivity.

By performing BD simulations with a simplified calcium channel model, we have been able to reproduce the remarkable properties of this channel. We find that the model is fairly sensitive to departures from the chosen structure. For example, if the radius of the selectivity filter is much larger than 2.8 Å, the presence of $Ca^{2+}$ ions fails to block the passage of $Na^+$ ions, as incoming ions can pass around the blocking ion. The mutation data cannot be reproduced in simulations if glutamate residues form a symmetrical ring, rather than being spread asymmetrically; and the behavior in mixed solutions cannot be reproduced if the filter is moved much further into the channel. Our model demonstrates how the complex behavior of the calcium channel can arise from simple electrostatic interactions between ions, the channel boundary and the charges therein.

This work was supported by grants from the Australian Research Council and the National Health and Medical Research Council of Australia. Calculations were done on the Fujitsu VPP-300 and the Linux alpha cluster of the ANU Supercomputer Facility.

## References

[1] R.W. Tsien, P. Hess, E.W. McClesky, R.L. Rosenberg, Annu. Rev. Biophys. Chem. 16 (1987) 265–290.
[2] D.A. Doyle, J.M. Cabral, R.A. Pfuetzner, A. Kuo, J.M. Gulbis, S.L. Cohen, B.T. Chait, R. MacKinnon, Science 280 (1998) 69–77.
[3] G. Chang, R.H. Spencer, A.T. Lee, M.T. Barclay, D.C. Rees, Science 282 (1998) 2220–2226.
[4] T.W. Allen, M. Hoyles, S. Kuyucak, S.H. Chung, Chem. Phys. Lett. 313 (1999) 358–365.

[5] T.W. Allen, A. Bliznyuk, A.P. Rendell, S. Kuyucak, S.H. Chung, J. Chem. Phys. 112 (2000) 8191–8204.
[6] I.H. Shrivastava, C.E. Capener, L.R. Forrest, M.S.P. Sansom, Biophys. J. 78 (2000) 79–92.
[7] E.W. McCleskey, W. Almers, Proc. Natl. Acad. Sci. USA 82 (1985) 7149–7153.
[8] C.C. Kuo, P. Hess, Neuron 9 (1992) 515–526.
[9] C.C. Kuo, P. Hess, J. Physiol. 466 (1993) 629–655.
[10] J. Yang, P.T. Ellinor, W.A. Sather, J.F. Zhang, R.W. Tsien, Nature 366 (1993) 158–161.
[11] A. Bahinski, A. Yatani, G. Mikala, S. Tang, S. Yamamoto, A. Scwartz, Mol. Cell. Biochem. 166 (1997) 125–134.
[12] A. Mikami, K. Imoto, T. Tanabe, T. Niidome, Y. Mori, H. Takeshima, S. Narumiya, S. Numa, Nature 340 (1989) 230–233.
[13] H.R. Guy, S.R. Durell, Soc. Gen. Physiol. Ser. 50 (1995) 1–16.
[14] S.W. Doughty, F.E. Blaney, W.G. Richards, J. Mol. Graph. 13 (1995) 342–348.
[15] S.H. Chung, T.W. Allen, M. Hoyles, S. Kuyucak, Biophys. J. 77 (1999) 2517–2533.
[16] M. Hoyles, S. Kuyucak, S.H. Chung, Comput. Phys. Commun. 115 (1998) 45–68.
[17] X.H. Chen, I. Bezprozvanny, R.W. Tsien, J. Gen. Physiol. 108 (1996) 363–374.
[18] T.W. Allen, S. Kuyucak, S.H. Chung, Biophys. Chem. 86 (2000) 1–14.
[19] R.L. Rosenberg, P. Hess, J.P. Reeves, H. Smilowitz, R.W. Tsien, Science 231 (1986) 1564–1566.
[20] R.L. Rosenberg, X.H. Chen, J. Gen. Physiol. 97 (1991) 1207–1225.
[21] P. Hess, J.B. Lansman, R.W. Tsien, J. Gen. Physiol. 88 (1986) 293–319.
[22] W. Almers, E.W. McCleskey, P.T. Palade, J. Physiol. 353 (1984) 565–583.
[23] T.X. Dang, E.W. McClesky, J. Gen. Physiol. 111 (1998) 185–193.
[24] C.C. Kuo, P. Hess, J. Physiol. 466 (1993) 657–682.
[25] L. Polo-Parada, S.J. Korn, J. Gen. Physiol. 109 (1997) 693–702.